OR-10-027

Investigation of Anticipatory Control Strategies in a Net-Zero Energy Solar House

José A. Candanedo
Student Member ASHRAE

Andreas K. Athienitis, PhD, PEng
Member ASHRAE

ABSTRACT

This paper investigates anticipatory control strategies in a house designed to have approximately net zero average annual energy consumption. These strategies are particularly useful in the case of optimized solar buildings, which include one or more of the following features: (a) passive solar design; (b) active systems for collection and control of solar energy (BIPV or BIPV/T systems, solar thermal collectors, motorized blinds); and (c) thermal energy storage systems (water tanks, phase change material containers). At the supervisory control level, prediction of future conditions can be employed to optimize the collection, storage and utilization of solar and geothermal energy. At a lower control level, predictive control assists in dealing with the discrepancies between the time constants of the building structure and its HVAC system, allowing the prescribed set-points to be reached when desired. This paper presents results of simulations which model the performance of a net-zero energy solar demonstration house using anticipatory control techniques. A relatively simple thermal network model is used throughout the building's design and in the development of the control strategies.

INTRODUCTION

Net-Zero Energy Solar Buildings

Buildings using both passive solar design techniques and active solar technologies integrated into the building envelope for collecting solar energy as electricity, heat and daylight are described here as "solar-optimized buildings". Through optimized design and operation, solar buildings may achieve net-zero annual energy consumption (i.e., they generate as much energy as they consume over the course of a year). This is usually accomplished by connecting the building to the electrical utility grid: when the generation of the building's renewable electricity system (usually photovoltaic panels) exceeds the building's consumption, the surplus is delivered to the grid. Conversely, when the power generation is insufficient for the building's needs, electric power is drawn from the utility grid. This configuration permits the use of the utility grid as an electric energy storage system. Net-zero energy solar buildings (NZESB) have recently become the focus of coordinated international research efforts (IEA-SHC 2008).

Anticipatory Control Strategies and Their Application to Solar-Optimized Buildings

Anticipatory control strategies for buildings, based on weather and load forecasting, have been proposed and studied as a suitable alternative to conventional control for the past quarter century (Winn and Winn 1985; Scartezzini et al. 1987; Kintner-Meyer and Emery 1995; Henze et al. 1997; Henze et al. 2005). In the '80s and early '90s, the lack of readily available weather forecasts represented a limitation for the development of these control strategies. This difficulty has been addressed by approaches such as manually introducing limited weather data complemented with historical records (Chen 1997), or by stochastic methods estimating the likelihood of a future weather pattern based on the current conditions (Nygård-Ferguson and Scartezzini 1992). Today, the availability of accurate weather forecasts online has opened up new possibilities for the use of anticipatory control strategies in buildings.

Solar-optimized buildings have several features that increase the potential of anticipatory control strategies for cold climates:

J.A. Candanedo is a PhD Candidate at the Department of Building, Civil and Environmental Engineering at Concordia University in Montréal, Canada. **A.K. Athienitis** is a Professor in the Department of Building, Civil and Environmental Engineering, and the Scientific Director of the Canadian Solar Buildings Research Network.

- First, passive solar design in heating-dominated climates requires proper orientation and geometry, adequate insulation, thermal mass and air-tightness, as well as larger than usual fenestration areas with high solar heat gain coefficient and low thermal conductance. These characteristics reduce the impact of exterior air temperature and make solar heat gains the most important factor affecting room interior temperature fluctuations. Predictive control can help to maximize the usefulness of the solar heat gains while preventing overheating through the use of the building's thermal mass to store thermal energy. Predictive control can also help in reducing electrical peak loads. Although predictive control has been mostly applied in cooling-dominated buildings (Braun et al. 1990), it is also appropriate when electric energy is used directly or indirectly for heating.
- Second, solar-optimized buildings include technologies that allow active collection of solar energy such as building-integrated photovoltaic (BIPV) modules, BIPV/thermal systems—used for electricity generation and collection of thermal energy (Bazilian et al. 2001)—solar thermal collectors and solar-assisted heat pumps. Although these technologies permit collecting large amounts of energy, their operation often requires a significant energy input (e.g., heat pump compressors require electric power in the order of kW). In consequence, their use should be planned in order to minimize net energy consumption and possibly peak loads as well. Other technologies, like switchable glazing and motorized blinds, allow a certain degree of control over solar heat gains, and therefore a certain control of the "charging" of the distributed thermal mass of the building.
- Third, thermal energy storage (TES) systems, such as water tanks or phase change materials (PCMs), may significantly help to reduce the problem of mismatch between the times of energy collection and use. An anticipatory control system becomes essential to handle the energy storage inventory.

In summary, anticipatory control techniques may be most useful in solar-optimized buildings, as they considerably reduce the impact of solar irradiance variations. Large-scale implementation of grid-connected solar-optimized buildings may offer significant benefits for electric utilities in terms of load management.

Figure 1A shows an example of a solar-optimized house. The passive solar design is largely determined by geometric parameters such as window-to-wall areas, "compactness" (ratio of exposed surface area to heated volume) of the building construction, and position and dimension of the overhangs. Passive solar design is complemented by active solar technologies. These active systems may be components such as building integrated photovoltaic/thermal (BIPV/T) systems, solar thermal collectors and controllable motorized blinds. Thermal energy storage (TES) is carried out passively (i.e., storage of the solar heat gains in the buildings' thermal mass) as well as actively in the TES device and the DHW tank. It may also be possible to actively charge the thermal mass of the building, for example, with a radiant floor heating (RFH) system. The numerous possibilities for thermal energy transfer and storage between the components of a solar-optimized house (Figure 1B) make a predictive control strategy highly desirable.

Applications of Anticipatory Control

Control may refer to two distinct, but closely related, control levels (ASHRAE 2007):

Supervisory control. This is usually done by establishing a schedule of set-points for room temperatures and other variables (e.g., humidity, state of charge of a TES device). Conventional approaches include maintaining a fixed set-point, using a different nocturnal set-point, or using several set-points throughout the day. An estimation of future loads

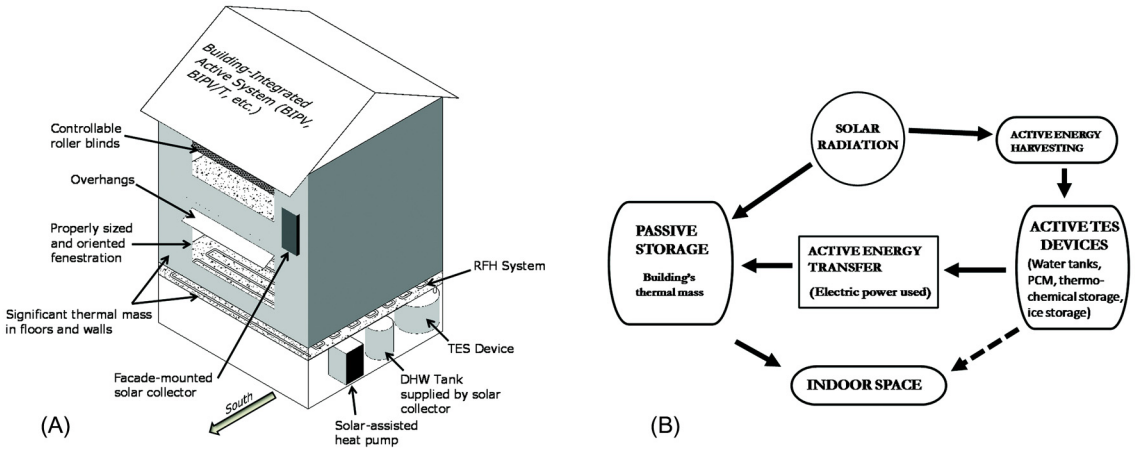

Figure 1 *(A) Generic solar-optimized house concept and (B) possibilities of thermal energy storage and energy transfer.*

(especially over a relatively long prediction horizon), can be very useful in planning the collection, storage and delivery of energy. One way to accomplish this is to use *optimal control theory*, a group of mathematical techniques used to find the control actions that will optimize an objective function (usually energy consumption, peak demand or cost) within a set of constraints. Optimal control techniques have been proposed to manage the building thermal mass (Braun 1990; Morris et al. 1994), the use of ice storage systems (Henze 1997), or the coordination of both passive and active storage (Kintner-Meyer and Emery 1995; Henze et al. 2004). Similar methods using simple model-based approach and system-identification have recently been proposed by Lee and Braun (2004, 2006, 2008).

Lower control level. If no corrective measures are taken, the differences between the time constants of the building's thermal mass, the HVAC system and the instrumentation will introduce significant time delays (on the order of hours) when attempting to follow the set-points prescribed by the supervisory control level (Athienitis et al. 1990). Although close set-point tracking is desirable, a certain degree of fluctuation is tolerated if human comfort is maintained. A technique known as "model predictive control", which uses a dynamic model of the system and expected inputs, has been used by Dexter and Haves (1989), Chen and Athienitis (1996), and Chen (2002). Adaptive control based on neural networks has also been used in lower-level control (Curtiss et al. 1996; Argiriou et al. 2000).

There have been relatively few investigations on the application of optimal control to residential solar buildings (Winn and Winn 1985; Nygård-Ferguson and Scartezzini 1989, 1992; Chen 2001). Most work on the management of passive and active storage has dealt with large commercial buildings, which are mostly cooling-dominated. Solar-optimized detached residential buildings, especially in cool climates, are often heating-dominated, and therefore management of the TES devices must be incorporated in the control strategies. Active envelope components such as motorized blinds and renewable energy systems should also be considered within the overall control strategy. Frequently updated, increasingly accurate and informative weather forecasts may now be readily incorporated in these control strategies (CMC 2007). Finally, anticipatory control can significantly contribute to reducing the dependence on external energy sources, thus contributing to the net-zero energy goal.

This paper presents the result of simulations carried out to model the use of anticipatory control strategies for a case study of a solar-optimized house.

CASE STUDY

The simulations presented here correspond to the Alstonvale Net Zero Energy Solar House (ANZESH), a solar-optimized house currently in an advanced phase of construction in the town of Hudson (45°27′N, 74°08′W) in the vicinity of Montréal (Figure 2). This 2470 ft^2 (230 m^2) house was designed as an entry of the *EQuilibrium Initiative*, a Canadian design competition of advanced residential buildings (CMHC 2008). Passive solar design plays an important role in this house. Table 1 presents the design insulation values, and Table 2 gives the fenestration areas in each façade.

Figure 2 *Construction of the Alstonvale Net Zero Energy Solar House.*

Table 1. Building Envelope Values of the Alstonvale Net Zero Energy Solar House

Building Envelope Component	R-Value (°F·h·ft^2·Btu^{-1})	RSI (m^2·KW^{-1})
Exterior walls	32	5.6
Ceiling	68	12.0
Concrete slab	26	4.6
Basement floor	26	4.6
Foundation walls	32	5.6

Table 2. Fenestration Areas in the Alstonvale Net Zero Energy Solar House

	Total Façade Area	Window Area	Window/Wall Ratio
South	1,313 ft^2 (122 m^2)	538 ft^2 (50 m^2)	41%
North	1,313 ft^2 (122 m^2)	0.0 ft^2 (0.0 m^2)	0%
East	721 ft^2 (67 m^2)	59.2 ft^2 (5.5 m^2)	8%
West	602 ft^2 (56 m^2)	60.2 ft^2 (5.6 m^2)	10%

Most of the main floor of the house consists of a concrete slab-on-grade 6 in (15 cm) thick. The rest of the habitable space of the floor consists of a 2-in (5-cm) layer of concrete on top of a wooden structure. A radiant floor heating system will be used to deliver heat to the space.

The simulations performed during the design process were carried out using several software tools. HOT2000 (NRCan 2008a) was used to perform a preliminary estimation of the heating and cooling loads, and to choose the levels of insulation of the building envelope. The auxiliary heating

energy for the house was calculated to be 22,970 MJ (21,768 kBtu) per year. The annual cooling load, according to HOT2000, has been estimated as 808 MJ (765 kBtu) for a summer set-point of 25.6°C (78.1°F). A solar chimney (which can be seen in Figure 2) has been installed to enhance natural convection effects and to eliminate the need for mechanical cooling.

The principal energy system of the ANZESH is its BIPV/T roof (Figure 3). Forty-two (42) photovoltaic panels with a nominal peak generating capacity of 7.35 kW_p at standard test conditions cover the lower two-thirds of the total roof surface (1130 ft^2, 105 m^2). Calculations carried out with RETScreen (NRCan 2008b) indicate that this system can provide a total yearly generation of 9,014 kWh. Rectangular glazing boards occupy the area of the roof not covered by the photovoltaic panels. The original design of the house included a smaller photovoltaic generation capacity (5.8 kW); it was increased to provide electric energy supply for an electric vehicle (Pogharian et al. 2008). The project now also includes a greenhouse for local food production.

A variable speed fan is used to draw air through the channel formed by the photovoltaic panels and the glass section (on top) and an insulated absorber surface (bottom). The air moving through the channel extracts thermal energy from the PV panels that would otherwise be lost to the exterior and increases the electrical efficiency of the panels; its temperature rises as it moves up the roof. Since most of the incident solar radiation can pass through the glazing and be received directly by the absorber surface, the glazing section significantly increases the air temperature. The air flow rates will vary between 470 to 850 L/s (1000 to 1800 CFM). A mathematical model was developed by dividing the channel into several sections (control volumes), and applying a one-dimensional energy balance in each section. The model was solved numerically, using solar radiation, air flow rates, exterior temperature, wind speed and sky temperature as inputs. Results indicate that on a clear sunny day in late February (1000 W/m^2 of normal incident solar radiation) with low wind speeds, and moderate flow rates, it is possible to increase the air temperature by up to 40°C (72°F) above the exterior air temperature. For a flow rate of 707 L/s (1500 CFM), this temperature rise corresponds to extracting 36 kW (123,000 Btu/h) of heat from the roof.

A BIPV/T system can significantly raise the temperature of the air passing through it. However, during winter in cold climates, the BIPV/T outlet air may not be hot enough for its direct practical application. This problem can be largely circumvented by using heat pumps to raise the quality of the available thermal energy (Bakker et al. 2005; Zondag 2005).

Because of shorter winter days and fluctuations in received solar energy, adequate conditions for the recovery of thermal energy with a heat pump are typically met only during a few hours per day, in which a large amount of thermal energy may be recovered. For this reason, thermal energy storage is essential in the implementation of BIPV/T systems. Often, these TES systems are "active" (i.e., the energy charge and discharge are subject to control). Active elements include water tanks, phase change material containers or thermochemical storage devices (Dincer 2002; Nielsen 2003).

The hot air leaving the BIPV/T system is collected by a manifold and conducted through two parallel ducts to an air-to-water heat exchanger in the ceiling of the garage, next to the mechanical room. The thermal energy from the air is then used to heat up a charge a a 1060-gal (4000-L) thermal energy storage (TES) water tank. The TES tank is charged through 4 modes of operation (Figure 4), in a configuration which will essentially be a solar/ground-loop hybrid heat pump.

The simplest mode of operation (**Mode A**) consists of direct heat transfer from the heat exchanger to the TES tank if the BIPV/T air temperature is high enough (i.e., at least a few degrees higher than the bottom of the tank).

If the BIPV/T air temperature is lower than that of the bottom of the tank, the BIPV/T air can be used as the source of two water-to-water heat pumps operating in parallel (Candanedo and Athienitis 2008a), which are used to charge the ANZESH active TES system. The operation of either both heat pumps (**Mode B**) or only one of them (**Mode C**) depends on the thermal energy available in the BIPV/T air.

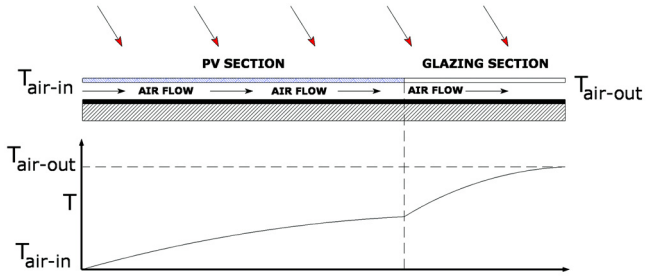

Figure 3 *BIPV/T System on the Alstonvale Net Zero Energy Solar House with typical temperature rise curve (actual surface is inclined 45° from the horizontal).*

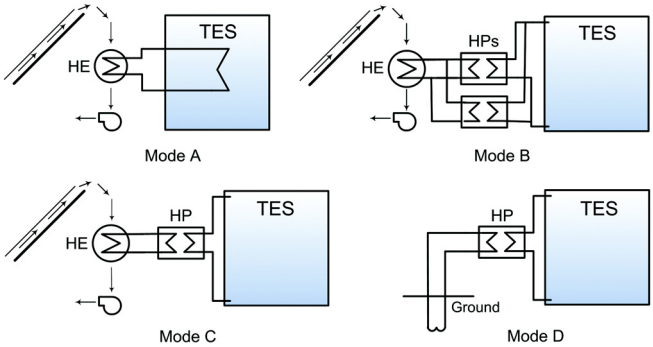

Figure 4 *Modes of charging the TES tank: Mode A (direct heat exchange), Mode B (BIPV/T air + 2 heat pumps), Mode C (BIPV/T air + one heat pump), and Mode D (ground source + heat pump).*

When the BIPV/T air temperatures are too low (e.g., less than 5°C or 41°F), the heat pump(s) can use a ground-loop as a backup source of thermal energy to charge the TES tank (**Mode D**).

It is proposed here that a mechanical system based on the use of thermal energy extracted from a BIPV/T installation may be used to supply most of the required heating needs of a house subjected to the rigorous winter conditions of Montréal. To facilitate this goal, anticipatory control algorithms were developed to optimize the collection, storage and delivery of the thermal energy. Although the simulations were applied to a specific case study, a similar approach may be followed in solar buildings having thermal storage capabilities.

The mechanical system (summarized in Figure 5) also includes a 40-tube evacuated tube solar collector mounted on the overhangs of the south façade and connected to a 400-L (106-gal) domestic hot water (DHW) tank. Water conservation measures (faucets with aerators, low flow showers, and low-consumption dual-flush toilets) significantly contribute to reducing the energy consumed for domestic hot water, estimated to be 160 L/day (42 gal/day). Water from the municipal mains will pass through a heat exchanger, wrapped around the gray water drain pipe from the shower, to recover thermal energy that would otherwise be lost. Simulations carried out in RETScreen (NRCan 2007), taking into account the temperature rise with the drain heat exchanger indicate that this solar thermal collector will supply about 90% of the DHW needs (about 2500 kWh or 8500 kBtu according to RETScreen).

DYNAMIC SIMULATIONS

The mathematical programming tools MATLAB and Simulink (MATLAB's environment for dynamic simulations), are used to study the behavior of the mechanical systems and the house. MATLAB/Simulink has often been applied to building simulation (Riederer 2005). Simulink, which uses a modular approach of interconnecting blocks and a graphical display, has also been adapted especially for building control studies (Husaundee and Visier 1999). It is also possible to write subroutines or subprograms (called M-files) to model systems that are not available by default. Simulink is a useful tool for the modeling and simulation of the building and its systems, and in particular for testing advanced control strategies. Tools such as TRNSYS and ESP-r were considered for the analysis of this system; however, the use of several non-conventional renewable energy systems (open loop BIPV/T roof, the heat pumps operating in parallel) presented additional challenges in their implementation. This was particularly difficult in the case of predictive control.

The building has been modeled through a thermal network representation, focusing on specific elements of the building envelope and the building structure (Athienitis et al. 1990). For example, a node N associated with a control volume with certain thermal inertia is connected to adjacent nodes A and B by thermal resistances R_A and R_B. The energy balance equation for this node can be written as:

$$C_N \frac{dT_N}{dt} = \frac{T_A - T_N}{R_A} + \frac{T_B - T_N}{R_B} + \sum Q \qquad (1)$$

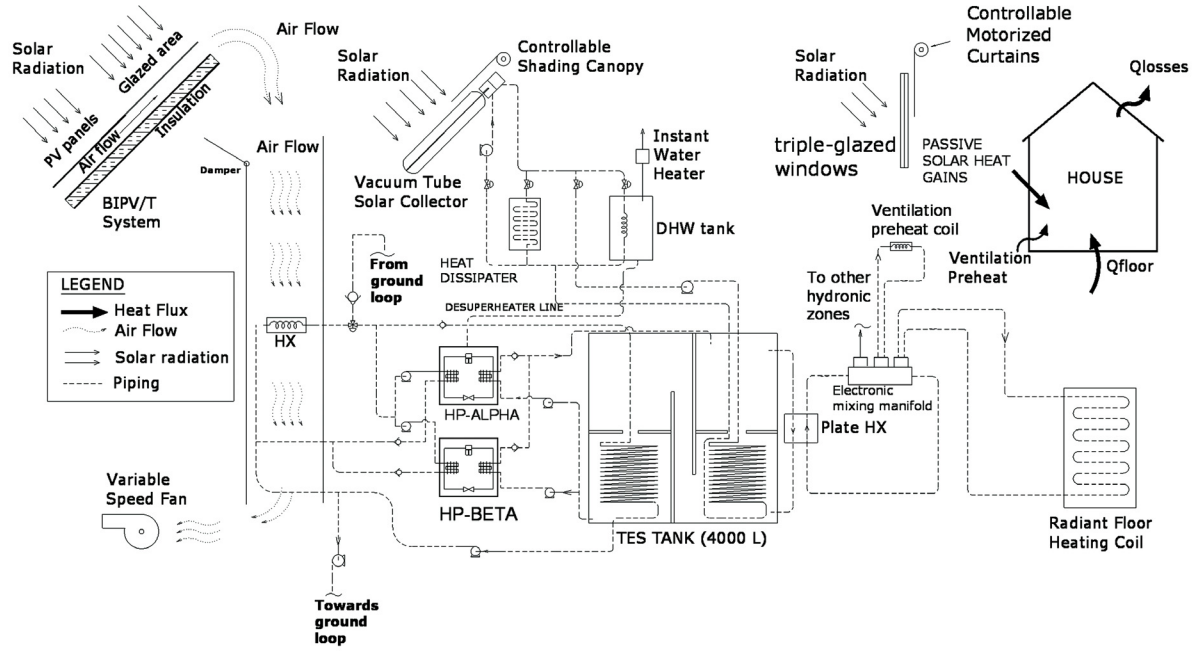

Figure 5 *Simplified schematic of the Alstonvale Net Zero Energy Solar House mechanical system.*

It has been shown that relatively few nodes provide a representation of the thermal response of the building which is good enough for some applications, such as the development of control algorithms (Athienitis et al. 1990).

Equation (1) can be written in Simulink by using the temperature of the neighboring nodes (T_A and T_B) as well as the summation of all additional energy sources as the inputs. The "heat contributions" are added and the result is divided by the capacitance of the node. An integrator operator is then used to calculate the node temperature (T_N) for the following time step as the output. This approach can be generalized for as many neighboring nodes and many additional heat sources as required. By following a similar procedure for each of the nodes in the thermal network, and connecting the different inputs and outputs from one block to the other, it is possible to represent the entire thermal network. In this case, a thermal network with 21 nodes has been used to represent the temperatures of the house. Simulink allows the use of several approaches for solving the equations in the system. Since many of the parameters change in a non-linear way, a fully explicit Euler method is used. A subprogram with values of several variables (capacitances, resistances, material properties, initial values, etc.) is included beforehand when opening the model.

The results of this model are comparable to the auxiliary heating energy calculated by HOT2000 (Table 3). The largest difference occurs in December, which is a particularly cloudy month in Montréal. Although the agreement is not quite perfect, Table 3 shows that the building model developed is adequate for studying different control strategies.

Apart from the blocks designed for the thermal modeling of the house, it is necessary to incorporate other mathematical models. Some of them are simple enough to be included directly in the graphical user interface file. The most complex models are written as independent subroutines (M-files), and can be invoked in the simulation as needed. Some of the modeling blocks written for this simulation include:

- **Sun's position and incidence angle calculations.** Based on the simulation time and the geographical coordinates of Montréal, the sun's position (solar altitude and azimuth) is calculated. This information is used to find incidence angles of the beam solar radiation on relevant surfaces of the ANZESH.
- **Radiation on different surfaces.** A subprogram with the Perez model (Perez et al. 1990) was used to calculate hourly solar radiation on different surfaces of the house corresponding to the weather file. The ground reflection was considered separately to account for the variation of ground reflectance throughout the year.
- **BIPV/T system.** This model uses a subprogram with the dimensions corresponding to the BIPV/T roof of the ANZESH. It includes the incoming solar radiation, the exterior temperature, a convective exterior heat transfer coefficient (based on wind speed), a radiative exterior heat transfer coefficient (based on equivalent sky temperature) and the air flow rate.
- **Heat Pump(s) model and heat exchanger.** A subprogram was written to find the heat transfer rate between the BIPV/T air and the water circulating through the air-to-water heat exchanger. This heat transfer rate should be approximately equal to the heat transfer taken by the heat pump group. This model is based on: (a) an approximate effectiveness equation (based on manufacturers' data) for the heat exchanger as a function of the flow rates, and (b) a look-up table corresponding to the technical specifications of the heat pump. This model calculates the heat delivered to the TES storage tank and the electrical consumption of the heat pumps. Details of this model were presented in Candanedo and Athienitis (2008a).
- **TES tank stratification.** The stratification in the thermal energy storage tank has been modeled with the multinode model described by Duffie and Beckman (2006a). In this case, the tank has been divided into 4 horizontal nodes. The flow coming from the heat pumps or from the flow rates will mix from the water in either of the nodes 1 to 4, depending on their temperature. The flow rates between nodes are calculated using mass flow balances. An accurate calculation of stratification in the TES tank would require more complex methods such as CFD simulations. However, it has been found that three or five nodes are usually enough for practical purposes (Duffie and Beckman 2006a). Although the heat pump(s) can deliver a large amount of energy (above 20 kW, or 68,200 Btu/h) to the water flow, a high flow rate is required and therefore the temperature rise created by the heat pump(s) is only between 5 and 10°C (9 and 18°F). Under these conditions, it is impossible to stratify the tank more than this temperature difference. Regardless, simulations indicate that the system operation remains satisfactory even in the worst case scenario (a fully mixed tank). It is expected that the link to the solar collector will contribute to stratify the tank.
- **Decision between modes of operation.** The mechanical system will charge the TES tank in the four different modes of operation shown in Figure 4. The decision to operate in a particular mode will depend on the temperatures of the TES tank and the BIPV/T air, and on the required set-point. The **ground source will be used only as a last resort**: even if the tank goes below the set-point, the ground source is only used if the bottom of the tank reaches a minimum allowable temperature (in this case, 28°C or 82.4°F).
- **Fan speed variation.** A simple scheme is used to change the fan speed according to the current solar radiation in a quasi-linear manner, leaning towards higher speeds since thermal efficiencies are higher under these conditions.

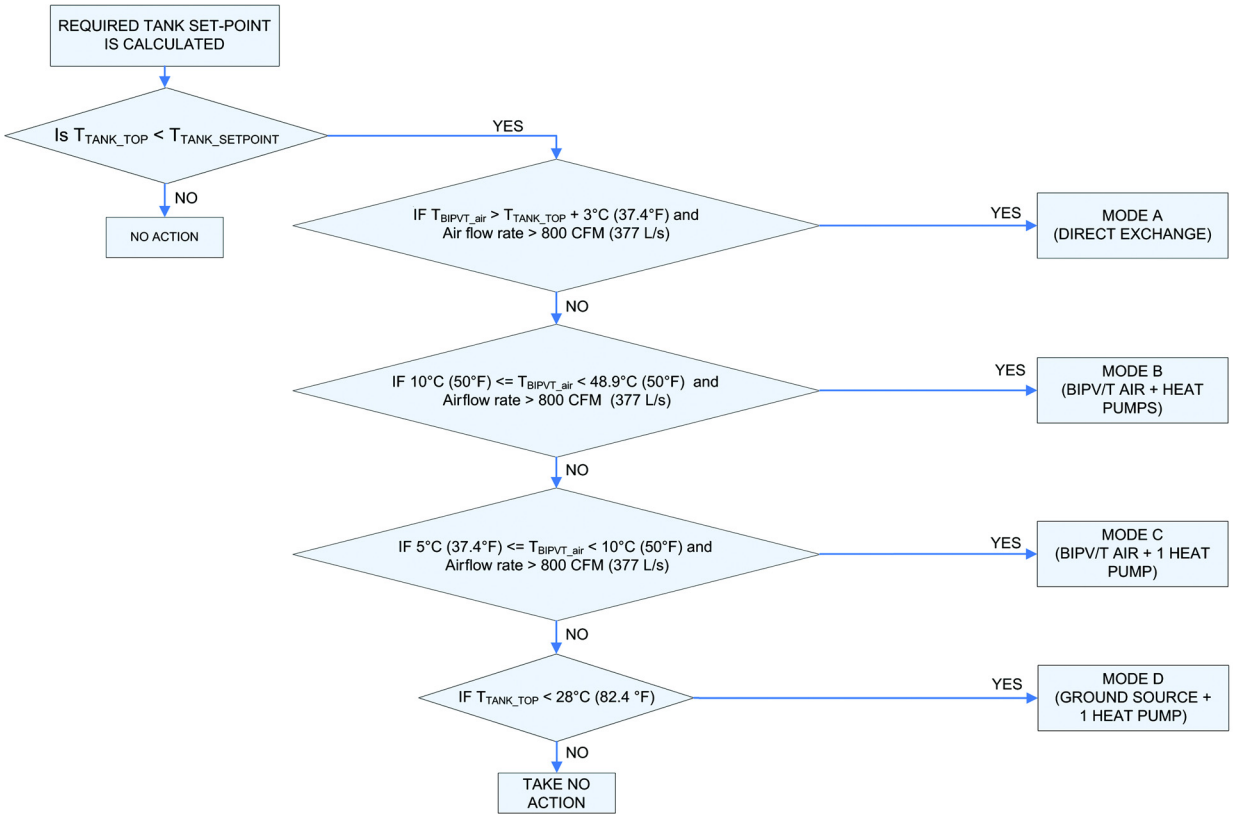

Figure 6 *Summary of the algorithm for selecting modes of operation.*

Table 3. Comparison of Heating Energy Estimated by the Current Model and HOT2000

	Current Model, MJ (kBtu)	HOT2000, MJ (kBtu)
December	9254 (8771)	6633 (6287)
January	5769 (5468)	6276 (5949)
February	5096 (4830)	4056 (3844)
March	2952 (2798)	2178 (2064)

$$\text{Fan Speed Control Signal} = \begin{cases} 0\%, \text{ if } T_{TANK\_TOP} \geq T_{TANK\_SETPOINT} \\ \text{else} \\ 100\%, \text{ if } S_{roof} > 950 \text{ W/m}^2 \\ 91.25\%, \text{ if } 800 \text{ W/m}^2 < S_{roof} \leq 950 \text{ W/m}^2 \\ 82.5\%, \text{ if } 500 \text{ W/m}^2 < S_{roof} \leq 800 \text{ W/m}^2 \\ 73.75\%, \text{ if } 300 \text{ W/m}^2 < S_{roof} \leq 500 \text{ W/m}^2 \\ 65\%, \text{ if } S_{roof} \leq 300 \text{W/m}^2 \text{ and } T_{ext} > 5°\text{C} \\ 0\%, \text{ if } S_{roof} \leq 300 \text{W/m}^2 \text{ and } T_{ext} \leq 5°\text{C} \end{cases} \quad (2)$$

- **Montreal weather** block. Simulink includes by default sinusoidal signals and other commonly used periodic functions, but other "forcing functions" can be defined as needed. Two different approaches were used:
- **Test sequences of five days** were designed to represent typical scenarios with different solar radiation conditions (Candanedo and Athienitis 2008b). In these sequences, sunny, intermediate and cloudy days were assigned a daily clearness index (K_T) of 0.7, 0.5 and 0.3, respectively (Duffie and Beckman 2006b). With this information, an hourly distribution of clearness indices was designed following the procedure described in Duffie and Beckman (2006b). The diffuse fraction of the global horizontal radiation was calculated according to Erbs et al. (1982). The last step was the calculation of radiation on surfaces with different orientations according to the model by Perez et al. (1990). The results presented in this paper correspond to a sequence of three sunny days followed by two cloudy days from January 15th to January 19th (solar angles were calculated accordingly). Exterior temperatures for Montréal were modelled using a steady-periodic curve using the design day data (quasi-sinusoidal) proposed by ASHRAE (2005) and an average value and fluctuation corresponding to January.

- Based on a **TMY2 (typical meteorological weather file)** for Montréal, signals were built for variables like dry bulb temperature, diffuse horizontal radiation, beam normal radiation, wind speed and others.

While annual weather data (TMY2 files) are useful for evaluating a system's performance during a month, a season or a year, the 5-day scenarios provide significant feedback for studying the effect of control strategies and their improvement.

The internal loads in this case were simulated, being conservative, with a constant source of 500 W (1700 Btu/h).

Finally, an important simplifying assumption is that the model used in the simulations does not include the interaction between the TES tank and the DHW loop with the solar collector. In the actual system, some heat transfer is expected to occur between both tanks, but it is expected that this will not be significant for the overall performance as both the space heating system and the DHW system have been designed to deal with their own loads nearly independently.

CONTROL STRATEGIES

Supervisory Predictive Control

The expected solar radiation for the current day and the following day (information available online) is used to decide on three variables: (a) the tank set-point; (b) the house temperature set-point; and (c) the blind position. This simple rule-based block has been designed to take advantage of solar energy by using the BIPV/T-heat pump(s)-TES group when conditions are favorable, and to manage the storage in the house thermal mass. For example, if it is sunny today, and cloudy conditions are expected tomorrow, then it is advisable to raise both the house and the TES set-points to increase the amount of stored thermal energy. Figure 7 shows the algorithm for modifying the set-points according to the expected solar radiation conditions.

The transmittance of the triple-glazed windows is calculated as a function of the beam incidence angle. To take advantage of solar heat gains while preventing overheating, the position of the blinds is adjusted based on the solar radiation expected for the current day, using weather data available at 6:00 AM [Equation (3)]. The effective transmittance (τ_{eff}) of the blinds is represented as a function of the position of the blinds.

$$\tau_{eff} = \begin{cases} 64\%, \text{ if } \mathrm{RAD}_{TODAY} > 10 \text{ MJ/m}^2, \text{ fully closed} \\ 76\%, \text{ if } 6.5 \text{ MJ/m}^2 < \mathrm{RAD}_{TODAY} \le 10 \text{ MJ/m}^2 \\ 88\%, \text{ if } 4.1 \text{ MJ/m}^2 < \mathrm{RAD}_{TODAY} \le 6.5 \text{ MJ/m}^2 \\ 100\%, \text{ if } \mathrm{RAD}_{TODAY} \le 4.1 \text{ MJ/m}^2, \text{ fully open blinds} \end{cases} \quad (3)$$

Lower-Level Control

Maintaining the house temperature within the set-point prescribed by the supervisory control is a challenging task because of the large time constants of the floor heating system and the building's thermal inertia in general. It has been decided that instead of following the traditional approach of imposing a constant set-point for specific times or ramp set-points, the building will be allowed to follow its natural oscillatory response, while keeping this oscillation within acceptable limits of human thermal comfort. The average value can be changed so that thermal energy can be stored from one day to the next. Therefore, the lower-control has been implemented in two steps:

- First, a sinusoidal curve with a period of one day is used as the house temperature set-point. The amplitude and average value of the curve are based on the expected solar radiation for the current day.

$$T_{house\_setpoint}(t) = Avg_{base} + Adj_{house} + Amp \cdot f_s \cdot \sin(\omega(t - t_a)) \quad (4)$$

where t is the current time (between 0 and 24 hours); t_a is a value used to displace the maximum point of the curve (in this case, t_a = 10.67 h, which sets the maximum temperature at 4:40 PM); Avg_{base} is the base average temperature (in this case, 21°C or 69.8°F); Adj_{house} is the adjustment of the average value according to the algorithm of Figure 7; Amp is half of the peak-to-peak amplitude of the temperature fluctuation (in this case, Amp = 2.75°C or 4.95°F); and f_S is a "swing factor" that is used to adjust the magnitude of the fluctuation depending on the expected total solar radiation. The Amp value was chosen from an estimation of the indoor temperature fluctuation for a sunny day with a partially closed blind or curtain having an effective transmittance of 88%, following a procedure similar to the one presented by Candanedo et al. (2007). The swing factor (f_S) is calculated as follows:

$$f_S = \frac{\tau_{eff}\,\mathrm{RAD}_{TODAY}}{(20\mathrm{MJ/m^2})(0.88)} \quad (5)$$

where τ_{eff} is the effective transmittance calculated according to Equation (3) and RAD_{TODAY} is the integration over the next 24 hours of the incident radiation on the roof.

- Second, a simple proportional control loop was used to control the heat delivery to the house comparing the current temperature to the set-point corresponding to a future time:

$$Q_{aux}(t) = K_P(T_{setpoint}(t + t_{ahead}) - T_{air}(t) + \Delta T_{offset}) \quad (6)$$

where $Q_{aux}(t)$ is the heat supplied at time t; K_P is the gain (W/°C); t_{ahead} is the "look-ahead" time (10 hours in

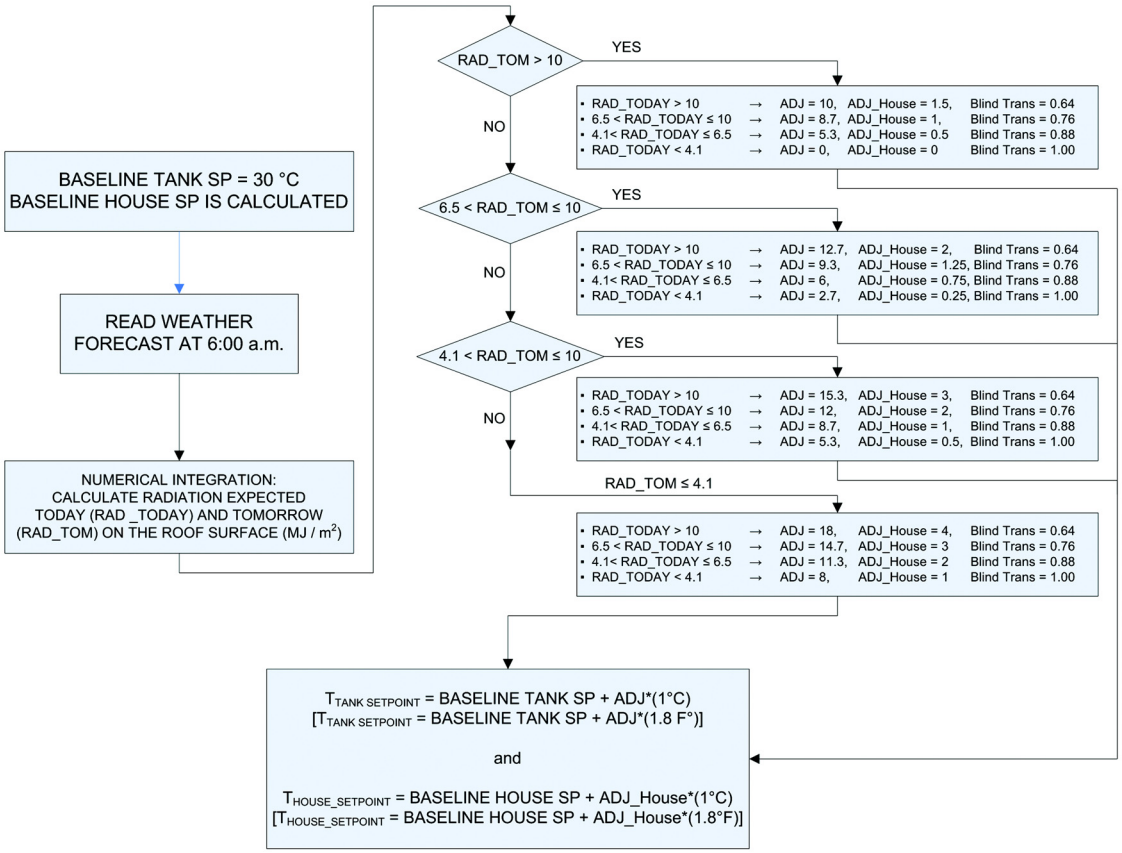

Figure 7 *Adjustment of tank and house set-points based on weather forecast data. Accumulated solar radiation is given in MJ/m² (1 MJ/m² = 88 Btu/ft²).*

this case); and ΔT_{offset} is used to correct the offset expected with proportional control (ΔT_{offset} = 2°C, or 3.6°F in these simulations). A lower limit of 0 kW (i.e., no cooling) was imposed, as well as an upper limit of 10 kW (34,100 Btu/h, the peak capacity of the system).

As a final measure to prevent overheating, it is assumed that the air changes per hour are changed from 0.4 to 1.5 when the indoor air temperature exceeds 28.5°C (83.3°F).

RESULTS AND DISCUSSION

Figure 8 presents the results of the simulation of the aforementioned control strategy (Predictive Control with Blinds Position Adjustment, PCBPA), while Figure 9 shows the results of a similar control strategy, the only difference being that the blind-curtain remains fully open during the daytime (Predictive Control with Blinds Fully-Open, PCBFO). In both cases, the periodic temperature fluctuation with an overall rising trend indicates that there is an accumulation of thermal energy from one sunny day to the next. The temperatures of the air leaving the BIPV/T system are, as expected, a strong function of the solar radiation.

With "Blinds Position Control" the blinds are adjusted depending on the expected solar radiation thus preventing overheating at the end of the third consecutive sunny day. This approach has the disadvantage that more heat is required from the mechanical system. The constant drain of thermal energy prevents the TES tank from reaching the set-point.

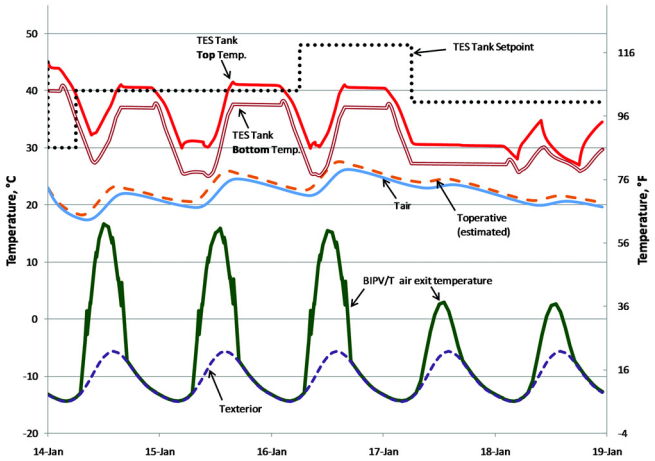

Figure 8 *TES tank set-point, and temperatures of the TES tank, indoor air, exterior air, BIPV/T exit air, and estimated operative temperature with blind position adjustment (Case A).*

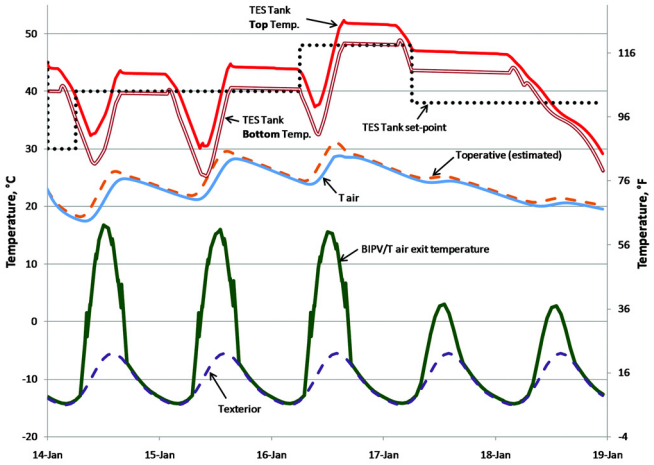

Figure 9 *TES tank set-point and temperatures of the TES tank, indoor air, exterior air, BIPV/T exit air, and estimated operative temperature with blinds fully open (Case B). The response with a fixed set-point at 21°C and proportional control is also shown as a reference.*

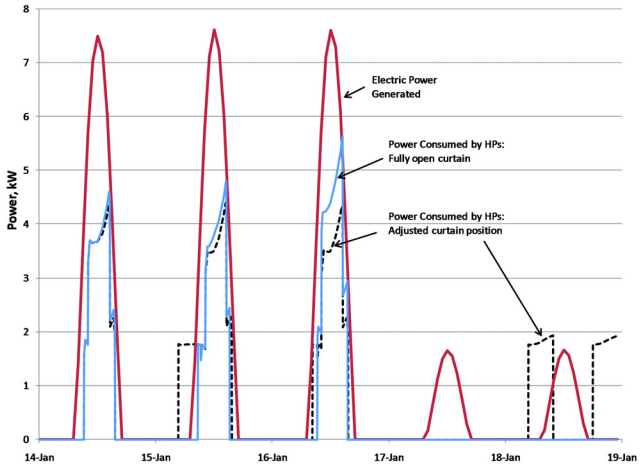

Figure 10 *Power generation with the corresponding heat pump consumption for the 5-day scenario with and without blind control.*

In the case of "Blinds Fully-Open" the house receives more energy from solar heat gains; the energy collected in the building's thermal mass and the TES tank prevents the use of the ground-source loop during the two cloudy days. During these two overcast days the house is heated with the energy accumulated during the preceding sunny days. The TES tank can easily reach the set-point, as it is not supplying heat to the house. However, it is clear that there are overheating problems on the second and third days. Figure 9 also shows the response using a fixed set-point of 21°C (69.8°F) with a proportional controller (2500 W/°C or 8530 Btu/h/°F). The temperature fluctuations are similar; however, at the fifth day the air temperatures are below 20°C (68°F) for about 10 hours.

Although it seems that "Blinds Position Control" strategy is preferable to "Blinds Fully-Open", the decision between one strategy or the other should also depend on the daytime occupancy.

Figure 10 shows the heat pump consumption for both control strategies, and the photovoltaic power generation (nearly identical for both conditions). As expected, the heat pump system is needed less when the blinds are kept fully open. In this case, the BIPV/T electric generation exceeds the heat pump power consumption at all times.

As the TES tank temperature increases, the heat pumps coefficient of performance (COP) decreases, and therefore more electric power is needed. When the position of the blinds is controlled, the ground source loop is used in the early hours of the morning of January 15th and 18th, as well as on the evening of January 18th. In comparison, when the blinds are kept fully open, the heat pumps are used less often, and only to extract heat from the BIPV/T air. Despite the lower energy consumption associated with keeping the blinds open, it is interesting to observe that a peak of electrical demand occurs in the afternoon of January 16th, during which more than 5 kW are required when the TES tank approaches its maximum state of charge.

Table 4 presents relevant electrical generation and consumption data for both cases. Table 5 presents the contribution of each mode to charging the TES tank.

Figure 11 shows the response of the house for the conditions of ten days in January, under the PCBPA strategy. The air temperature tends to follow approximately the shape of the set-point: however, the fluctuations of the indoor temperature are smaller than those of the set-point. At the beginning of the simulation, the air temperature is rather low before reaching steady state, but in general the temperatures of the house are quite satisfactory, especially if surface temperatures are used to estimate the operative temperature (ASHRAE 2005). Figure 12 shows the operative temperature and the tank set-point of the house for ten days in March. It can be seen that the control system raises the tank set-point when a sunny day precedes a cloudy day.

IMPLEMENTATION AND MONITORING

The control strategies presented here are based on the current possibility of downloading weather forecasts every 12 hours from the Environment Canada website. A DOS script was written to carry out this task. In preparation of this implementation, a program is used to analyze the information provided. The Perez model (Perez 1990) is used to calculate the expected irradiance on any surface of interest, such as the BIPV/T roof and the fenestration.

These strategies will be experimentally tested in the Alstonvale Net Zero Energy Solar House when its construction is completed later this year. The Alstonvale Net Zero

Table 4. Electric Energy Generated by the BIPV/T System and Consumed by the Heat Pumps

	Predictive Control with Blinds Position Adjustment	Predictive Control with Blinds Fully Open
Electric energy generated	152.5 kWh	152.5 kWh
Electric energy consumed by HPs	89.5 kWh	67.8 kWh

Table 5. Energy Delivered by the Mechanical System to the TES Tank in the Four Modes of Operation

Heat Delivered – Mode	Predictive Control with Blinds Position Adjustment, MJ (kBtu)	Predictive Control with Blinds Fully Open, MJ (kBtu)
A	0 (0)	0 (0)
B	765 (725)	765 (725)
C	164.9 (156.3)	150.5 (142.6)
D	522.7 (495.4)	20.5 (19.4)

Energy Solar House will be monitored by several independent parties: more than 200 variables will be measured. The control algorithms presented here will be implemented and tested in the house.

CONCLUSIONS

The investigation presented here demonstrates that weather forecasts of expected solar radiation can be successfully used to manage the collection, storage and delivery of thermal energy from a BIPV/T system. Careful planning of the cycles of charge and discharge of the TES system allows operating the heat pumps in the high COP range. Improving the set-point sequence of the TES tank facilitates taking advantage of the solar energy when it is available, storing it for future use, and avoiding resorting to the ground-source loop which usually has a lower COP. It should be noted that an additional advantage to cooling the photovoltaic panels in the BIPV/T system is increased electricity production.

Solar radiation forecasts can also be used to adjust the position of south-facing blinds in order to prevent overheating inside the house. However, although adjusting the position of the blinds improves comfort, this action has repercussions on the amount of energy that can be stored in the distributed thermal mass, and therefore has an impact on the energy required from the heating system. Table 4 shows that the consumption of electric power by the heat pumps is noticeably higher for the period considered as compared to the case when the blinds are left fully open.

The set-points presented here for the TES tank and the house temperatures are based on simple look-up tables depending on the expected solar radiation for two consecutive days. This approach is not intended as an "optimal" control

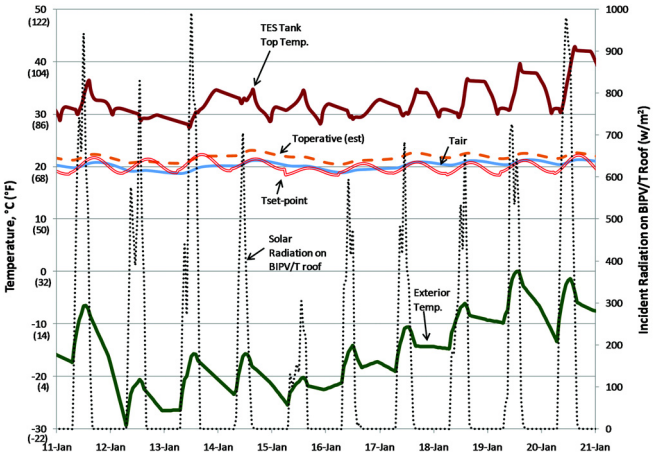

Figure 11 *TES tank top temperature and relevant indicators of thermal comfort (average surface temperature, indoor air temperature, and estimated operative temperature) for 10 days in January. Solar radiation and exterior temperature are presented as well.*

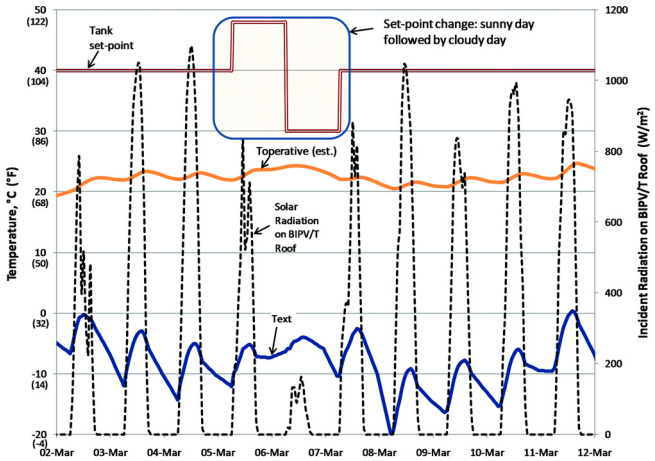

Figure 12 *TES tank set-point and estimated operative temperature for 10 days in March. Solar radiation and exterior temperature are presented as well.*

model predictive control, could improve the system's performance.

As mentioned before, in a solar-optimized house, solar radiation is the most important factor on the indoor temperature fluctuations. The strategies presented here use only solar radiation forecasts. However, a potential improvement for predictive control is the incorporation of temperature forecasts in the selection of set-points.

The configuration presented here does not rely completely on solar energy for its needs: a backup heating system (in this case a ground source loop) remains necessary.

Future designs of solar-optimized houses could significantly reduce the need for backup heat sources by optimizing the size of the active TES system, and properly managing active and passive thermal storage capacity.

ACKNOWLEDGMENTS

Funding and technical support have been provided by the Canadian Solar Buildings Research Network (SBRN) a strategic network of the Natural Sciences and Engineering Research Council of Canada (NSERC), and by CanmetENERGY Varennes (Natural Resources Canada) through the TEAM (Technology Early Action Measures) initiative. The support of Hydro Québec, CMHC and l'Agence de l'Efficacité Énergétique du Québec to the Alstonvale project is gratefully acknowledged. The first author would like to thank NSERC for financial support through a CGS Alexander Graham Bell Graduate Scholarship. We would like to thank Sevag Pogharian, the leader of the Alstonvale project, and all the members of the Alstonvale project design team for their ideas and contributions.

NOMENCLATURE

ADJ	Adjustment to TES tank set-point [°C]
Adj_{house} or ADJ_House	Adjustment to the indoor air set-point [°C]
Amp	Half of the peak-to-peak amplitude of the set-point fluctuation [°C]
Avg_{base}	Baseline average set-point temperature [°C]
C_N	Node capacitance [J/(kg·K)]
f_S	Swing factor
K_P	Proportional gain [W/°C]
K_T	Daily clearness index
Q	Heat flux entering node N [W]
$Q_{aux(t)}$	Auxiliary heating [W]
RAD_{TODAY} or RAD_TODAY	Radiation expected on the current day on the BIPV/T surface [MJ]
RAD_{TOM} or RAD_TOM	Radiation expected the next day on the BIPV/T surface [MJ]
R_A, R_B	Thermal resistances between A and N, and B and N [°C/W]
S_{roof}	Instant radiation on the BIPV/T roof [W/m^2]
t_a	Time displacement of the sinusoidal set-point curve [s]
t_{ahead}	"Look-ahead" time in the proportional control loop [s]
T_A, T_B	Temperature of nodes surrounding node N [°C]
T_{BIPVT_air}	Temperature of the air leaving the BIPV/T channel [°C]
$T_{house\_setpoint}(t)$	Indoor air set-point [°C]
T_N	Node temperature [°C]
T_{TANK_TOP}	Temperature of the top node of the TES tank [°C]
$T_{TANK\_SETPOINT}$	Set-point temperature of the TES tank [°C]

Greek Symbols

ΔT_{offset}	Offset temp in control loop [°C]
τ_{eff}	Effective blind transmittance
ω	Angular frequency corresponding to one cycle per day [rad/s]

Acronyms

ANZESH	Alstonvale Net Zero Energy Solar House
BIPV	Building-integrated photovoltaic system
BIPV/T	Building-integrated photovoltaic/thermal
CFD	Computational fluid dynamics
COP	Coefficient of performance
DHW	Domestic hot water
RFH	Radiant floor heating system
TES	Thermal energy storage
TMY2	Typical meteorological year file, version 2

REFERENCES

ASHRAE. 2005. *2005 ASHRAE Handbook—Fundamentals*. Atlanta: American Society of Heating, Refrigerating and Air-Conditioning Engineers, Inc.

ASHRAE. 2007. *2007 ASHRAE Handbook—HVAC applications*. Atlanta: American Society of Heating, Refrigerating and Air-Conditioning Engineers, Inc.

Athienitis, A.K., M. Stylianou, and J. Shou. 1990. A methodology for building thermal dynamics studies and control applications. *ASHRAE Transactions* 96(2):839-48.

Bakker, M., H.A. Zondag, M.J. Elswijk, K.J. Strootman, and M.J.M. Jong. 2005. Performance and costs of a roof-sized PV/thermal array combined with a ground coupled heat pump. *Solar Energy* **78**, 331-339.

Bazilian, M., N.K. Groenhout, and D. Prasad. 2001. Simplified numerical modeling and simulation of a photovoltaic heat recovery system. *17th European Photovoltaic Solar Energy Conference*. Munich, Germany.

Berdahl, P. and M. Martin. 1984. Emissivity of clear skies. *Solar Energy* 50:663-664.

Braun, J. 1990. Reducing energy costs and peak electrical demand through control of building thermal storage. *ASHRAE Transactions* 96(2):876-888.

Candanedo, J.A. and A.K. Athienitis. 2008. Simulation of the performance of a BIPV/T system coupled to a heat pump in a residential heating application, *9th International IEA Heat Pump Conference*, May 20-22. Zürich, Switzerland.

Candanedo, J.A. and Athienitis, A.K. 2008. Modeling of predictive control strategies in a net zero energy house with passive and active thermal storage, *EUROSUN2008*, October 7-10. Lisbon, Portugal.

Candanedo, J.A., B. O'Neill, S. Pantic, and A.K. Athienitis. 2007. Studies of control strategies at the concordia solar house, *Joint 2nd Solar Buildings Research Network—32nd Solar Energy Society of Canada Inc. (SESCI) Conference*, June 10-14. Calgary, Alberta.

CMHC. 2008. Canada Mortgage and Housing Corporation: *The five principles of EQuilibrium Housing*. http://www.cmhc-schl.gc.ca/en/inpr/su/eqho/eqho_001.cfm.

Chen, T. and A.K. Athienitis. 1996. Ambient temperature and solar radiation prediction for predictive control of HVAC systems and a methodology for optimal building heating dynamic operation. *ASHRAE Transactions* 102 (1):26-35.

Chen, T. 1997. *A methodology for thermal analysis and predictive control of building envelope heating systems*. PhD thesis, Concordia University, Montréal, Québec, Canada.

Chen, T. 2001. Real-time predictive supervisory operation of building thermal systems with thermal mass, *Energy and Buildings* 33(2):141-150.

Chen, T. 2002. Application of adaptive predictive control to a floor heating system with a large thermal lag. *Energy and Buildings* 34(1):45-51.

CMC. 2007. Canadian Meteorological Centre Product Guide http://collaboration.cmc.ec.gc.ca/cmc/cmoi/product_guide/table_of_contents_e.html.

Curtiss, P., G. Shavit, and J. Kreider. 1996. Neural networks applied to buildings: A tutorial and case studies in prediction and adaptive control. *ASHRAE Transactions* 102(1): 1141-1146.

Dexter, A. and P. Haves. 1989. A robust self-tuning predictive controller for HVAC applications. *ASHRAE Transactions* 95(2):431-438.

Dincer, I. 2002. On thermal energy storage systems and applications in buildings. *Energy and Buildings* 34(4): 377-388.

Duffie, J. and W. Beckman. 2006a. *Solar Engineering of Thermal Processes*, 3rd ed. Chapter 8.4, Energy storage: Stratification in storage tanks. John Wiley & Sons, Hoboken, NJ.

Duffie, J. and W. Beckman. 2006b. *Solar Engineering of Thermal Processes*, 3rd ed. Chapter 2.13, Estimation of hourly radiation from daily data. John Wiley & Sons, Hoboken, NJ.

Erbs, D.G., S.A. Klein, and J.A. Duffie. 1982. Estimation of diffuse radiation fraction for hourly, daily and monthly-average global radiation. *Solar Energy* 28:293.

Henze, G., R. Dodier, and M. Krarti. 1997. Development of a predictive optimal controller for thermal energy storage systems. *International Journal of HVAC&R Research* 3(3):233-264.

Henze, G., C. Felsmann, and G. Knabe. 2004. Evaluation of optimal control for active and passive building thermal storage. *International Journal of Thermal Sciences* 43(2):173-183.

Henze, G., D. Kalz, S. Liu, and C. Felsmann. 2005. Experimental analysis of model based predictive optimal control for active and passive building thermal storage inventory. *International Journal of HVAC&R Research* 11(2):189-213.

Husaundee, A.M.I., and J.-C. Visier. 1999. The building HVAC system in control engineering—A modeling approach in a widespread graphical environment. *ASHRAE Transactions* 105(1):319-329.

IEA-SHC. 2008. IEA-SHC Task 40—ECBCS Annex 52: Towards Net Zero Energy Solar Buildings. http://www.iea-shc.org/task40/index.html

Kintner-Meyer, M. and A. Emery. 1995. Optimal control of an HVAC system using cold storage and building thermal capacitance. *Energy and Buildings* 23(1):19-31.

Lee, K. and J. Braun. 2004. Development and application of an inverse building model for demand response of small commercial buildings. *Proceedings of SimBuild 2004, IBPSA-USA Conference*, Boulder, Colorado.

Lee K. and J. Braun. 2006. Development of methods for determining demand-limiting setpoint trajectories in commercial buildings using short-term data analysis. *Proceedings of SimBuild 2006, IBPSA-USA Conference*. Cambridge, MA.

Lee K. and J. Braun. 2008. Model-based demand-limiting control of building thermal mass. *Building and Environment* 43:1633-1646.

Morris, F., J. Braun, and S. Treado. 1994. Experimental and simulated performance of optimal control of building thermal storage. *ASHRAE Transactions* 100(1):402-414.

Nielsen, K. 2003. Thermal energy storage: A state-of-the-art. Report within the research program Smart Energy-Efficient Buildings at NTNU and SINTEF 2002-2006. Department of Geology and Mineral Resources Engineering, Norwegian University of Science and Technology, Trondheim, Norway.

NRCan. 2007. RETScreen International website. http://www.retscreen.net/.

NRCan. 2008a. Natural Resources Canada: HOT2000. http://oee.nrcan.gc.ca/residential/personal/new-homes/r-2000/standard/hot2000.cfm?attr=4.

NRCan. 2008b. Natural Resources Canada: RETScreen. http://www.retscreen.net/ang/home.php.

Nygård-Ferguson, M. and J.-L. Scartezzini. 1989. Computer simulation of an optimal stochastic controller applied to passive solar rooms. *Energy and Buildings* 14:1-7.

Nygård-Ferguson, M. and J.-L. Scartezzini. 1992. Evaluation of an optimal stochastic controller in a full-scale experiment. *Energy and Buildings* 18:1-10.

Perez, R., P. Ineichen, R. Seals, J. Michalsky, and R. Stewart. 1990. Modeling daylight availability and irradiance components from direct and global irradiance, *Solar Energy* 44(5):271-289.

Pogharian, S., J. Ayoub, J. Candanedo, and A.K. Athienitis. 2008. Getting to a net zero energy lifestyle in Canada: the Alstonvale Net Zero Energy Solar House, *23rd European PV Solar Energy Conference*. Valencia, Spain.

Riederer, P. 2005. MATLAB/Simulink for building and HVAC simulation—state of the art, *Ninth IBPSA Conference*, Montréal, Canada.

Scartezzini, J.-L., A. Faist, and T. Liebling. 1987. Using Markovian stochastic modeling to predict energy performance and thermal comfort of passive solar systems. *Energy and Buildings* 10(2):135-150.

Winn, R. and C. Winn. 1985. Optimal control of auxiliary heating of passive-solar-heated buildings. *Solar Energy* 35(5):419-428.

Zondag, H.A. 2005. Combined PV-air collector as heat pump air preheater. *Build It Solar website*. www.builditsolar.com/Projects/rx02065.pdf.